Spins of resonances in reactions of neutrons with ^{238}U and ^{113}Cd

F. Gunsing,* K. Athanassopulos, and F. Corvi
CEC-JRC, Institute for Reference Materials and Measurements, B-2440 Geel, Belgium

H. Postma
Delft University of Technology, P.O. Box 5046, NL-2600 GA Delft, The Netherlands

Yu. P. Popov and E. I. Sharapov
Joint Institute for Nuclear Research, 141980 Dubna, Moscow Region, Russia
(Received 14 March 1997)

In this paper experiments are described that have led to the assignment of spins of a large number of s- and p-wave resonances in reactions of epithermal neutrons with the nuclei ^{238}U and ^{113}Cd. The gamma-ray spectra of the (n,γ) reactions have been measured using the time-of-flight technique at the GELINA pulsed neutron source facility. For the present spin determinations we have exploited the fact that the population through gamma radiation of low-lying nuclear states from the compound nucleus is dependent on the resonance spin. These assignments are important for the analysis of measurements of parity nonconservation in compound nuclei. [S0556-2813(97)00909-6]

PACS number(s): 21.10.Hw, 25.40.Lw, 27.60.+j, 27.90.+b

I. INTRODUCTION

The knowledge of spins of compound nuclear states, formed by the reaction of epithermal neutrons with heavy mass target nuclei, has recently become of greater interest in relation to parity nonconservation (PNC) measurements in neutron resonances. Parity nonconservation, a property of the weak interaction, is strongly enhanced in epithermal neutron resonances due to the small level spacing and the large ratio of the neutron widths of s-wave resonances compared to those of p-wave resonances [1]. Whereas the ratio of the strength of the weak interaction to that of the strong interaction is about 10^{-7} in the nucleon-nucleon interaction, this enhancement may easily produce parity nonconservation effects of several percent in compound nucleus reactions.

PNC effects have been observed in several neutron resonances of the zero-spin target nuclei ^{238}U and ^{232}Th in the TRIPLE experiments at Los Alamos [2,3]. This made it possible to estimate the root mean squared parity nonconserving matrix element M in nuclear matter, a quantity that reveals the overall effective strength of the weak interaction in the nucleus. After the success for these heavy mass nuclei, work on parity nonconservation at p-wave resonances of spin-zero and spin nonzero nuclei in the mass region $A \simeq 110$ has been started and thus spin assignments of s- and p-wave resonances will remain of interest for some time to come [4,5]. It is believed that a corresponding amplification in the compound nucleus holds also for effects due to violation of time reversal invariance (TRI). Several experiments concerning the direct observation of TRI violation are currently considered by various groups and the knowledge of resonance spins is also of interest for these experiments, not only for the p-wave resonances but also for s-wave resonances.

The resonance spin J is the vector combination $\mathbf{J}=\mathbf{I}+\mathbf{s}+\mathbf{l}$ of the target nuclear spin I, the spin of the neutron $s=1/2$, and its orbital momentum l. Parity nonconservation is related to the $\mathbf{j}=\mathbf{s}+\mathbf{l}$ part at the entrance channel. For the zero-spin target nucleus ^{238}U only the $J^{\pi}=1/2^{-}$ p-wave resonances can be admixed by the $J^{\pi}=1/2^{+}$ s-wave resonances and show parity nonconservation. In the case of the $I=1/2$ target nucleus ^{113}Cd the $J=0$ p- and s-wave resonances can mix while the $J=1$ resonances mix partially depending on the $p_{1/2}$ fraction of the neutron entrance channel. The $J=2$ p-wave resonances cannot show parity nonconservation.

In order to correctly interpret the results of the parity nonconservation measurements, one needs to know the resonance spins. A spin assignment program has been initiated at the Institute for Reference Materials and Measurements (IRMM) in Geel, Belgium, using the pulsed neutron source GELINA. This project started with the determination of the neutron s- and p-wave resonances of the isotopes ^{238}U and ^{113}Cd using neutron-capture gamma-ray spectroscopy. Parts of this work have been published before in a preliminary form in conference reports and a Ph.D. thesis [6–9]. The final results are reported here. Currently, other isotopes are under investigation in Geel among which are ^{109}Ag [10] and ^{107}Ag.

II. METHODS TO ASSIGN NEUTRON RESONANCE SPINS

A. Spin assignment methods

Several methods have been applied in the past to assign the spins of neutron s-wave resonances. Some of them can only be applied in special cases. A rather general review is given by Mughabghab [11]. The most direct method is the transmission of polarized neutrons through targets of polarized nuclei. The difference in cross section due to the helicity

*Present address: CEA Saclay, F-91191 Gif-sur-Yvette, France. Electronic address: gunsing@cea.fr

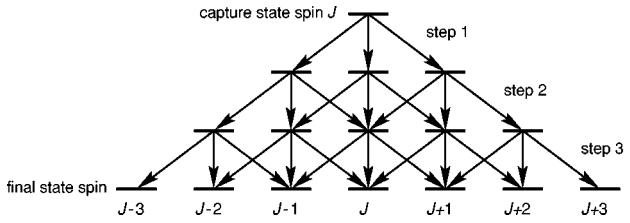

FIG. 1. The number of possible spin changes and states reached from the initial capture state after three steps.

of the neutrons can be used to determine the resonance spins. This has been successfully applied for s-wave resonances in, for example, the case of ^{235}U [12–14]. However, this method is limited to nuclei which can be polarized in substantial quantities. We remark that the transmission of polarized neutrons through polarized targets can also be used to assign spins to p-wave resonances and that both the spin and the channel spin mixing can be determined [15]. This kind of experiment is technically difficult to perform and of course, this method cannot be applied to nuclei with zero spin.

Of the other methods we mention the use of gamma rays following neutron capture, which is reported in this paper, and which has been shown to be useful and reliable in the case of both s- and p-wave resonances of ^{238}U and ^{113}Cd.

One can also exploit the spin dependence of the gamma multiplicity, which is the average number of gamma decay steps after neutron capture, necessary to reach the ground state. Coceva [16] used this for s-wave resonances in several $I=5/2$ and $I=7/2$ nuclei and Georgiev [17] assigned s-wave resonance spins of ^{179}Hf.

Another method to measure the resonance spins is to determine the spin statistical factor $g=(2J+1)/[2(2I+1)]$ which works well for nuclei with low spin values and with $A<60$ where the neutron width Γ_n is large. However, low-energy p-wave resonances in the heavy mass region have such small neutron widths that this method becomes practically impossible. For the same reason the angular distribution of elastically scattered neutrons is difficult to measure.

B. Resonance spin assignments based on secondary gamma rays using the low-lying level population method

At the GELINA facility we have mainly used the method of low-level population, based on secondary gamma rays. For medium and heavy mass nuclei there are many possible ways for the compound nucleus to decay through gamma radiation since the number of levels is very large between the ground state and the capture state. The decay of the nucleus can be treated within the statistical model. The population of low-lying nuclear states may depend significantly on the spin of the capture state.

The method can be illustrated with a simple example. Consider the decay of a capture state with spin J that decays through the emission of dipole radiation, as is mainly the case with statistical γ decay [18]. After each step in the cascade, the spin change is $\Delta J=-1,0,1$. After three steps all states with spins between $J-3$ and $J+3$ can be reached, as is illustrated in Fig. 1. For each step the branching ratio can be taken proportional to the spin dependent factor $f(J)$ of the level density, taken from [19]:

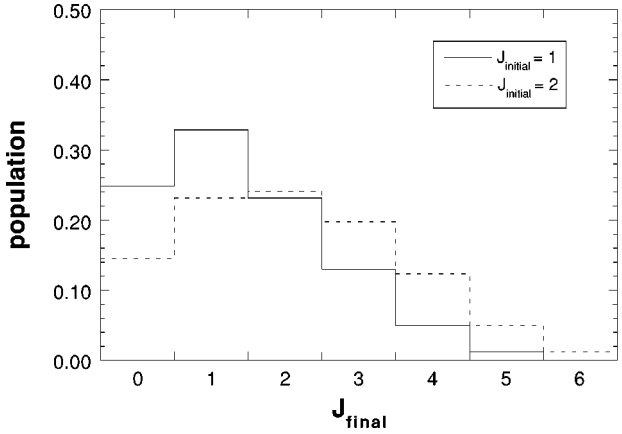

FIG. 2. The population of final spin states after the decay of a spin $J=1$ and a spin $J=2$ resonance state in four steps, using branching ratios based on the spin dependent factor of the level density.

$$f(J)=\exp\left(\frac{-J^2}{2\sigma_c^2}\right)-\exp\left(\frac{-(J+1)^2}{2\sigma_c^2}\right)$$
$$\simeq\frac{2J+1}{2\sigma_c^2}\exp\left(\frac{-(J+1/2)^2}{2\sigma_c^2}\right), \qquad (1)$$

where σ_c^2 is the spin cutoff factor. The factor $f(J)$ is proportional to $2J+1$ for low spins. A simple straightforward calculation gives the population of spin states after a certain number of steps where the cutoff factor can be taken, for example, from [20]. In Fig. 2 this is illustrated with the spin state populations after decay of a spin $J=1$ and a spin $J=2$ resonance state in four steps. Obviously, one has to select final levels with spins J_f differing from the initial resonance spin J, but the difference should not be too large as otherwise the population intensity will be too low. Of course, this way of proceeding is only a crude approximation. More realistic and detailed calculations, involving the event-by-event based Monte Carlo simulation of the decay of a specific excited nucleus, can be performed using the computer code DICEBOX, developed by Bečvář and Ulbig [21]. Such calculations have been performed for the case of ^{113}Cd [22] and found to be in good agreement with the experimental results presented here.

The resonance spin effect can be increased by observing the ratio of the populations of two final states with a spin, respectively, larger and smaller than the initial spins. An additional advantage of this ratio is that it does not need normalization to the total capture rate. The value of the ratio is dependent on the resonance spin and should, for a set of resonances, split into different groups for the various possible resonance spins. In an experiment, the populations of the levels are measured by investigating the intensities of the gamma rays depopulating them.

Although this method allows the determination of the spin of a resonance, it has recently been found that the low-level population may in some cases also depend on the parity of the capture state [23,24]. At epithermal neutron energies the strength of s waves is much larger than that of p-wave resonances. Therefore the s- or p-wave nature, and therefore its

parity, is often clear from the difference in Γ_n at low energies. At higher neutron energies this difference disappears and thus a parity effect on the populations of levels with the same spin but different parity might be useful to distinguish s- and p-wave resonances.

In the past years this low-level population method has been applied to a number of nuclei to determine the resonance spins of s waves [25–29]. The present extension to the case of p-wave resonances is straightforward though experimentally much more difficult because of the very weak strengths of most p-wave resonances compared to s-wave resonances at epithermal neutron energies. The measuring time may span several months and special care must be taken about background corrections if p- and s-wave resonances are close.

C. Resonance spin assignments based on primary gamma rays

Primary transitions, feeding low-lying levels of the excitation spectrum with known spin and parity, may also contribute information about resonance spins. Because the observed transitions usually have a dipole character, knowing the final spin I_f limits the resonance spin to be $J=I_f\pm 0,1$. Although $E2$ radiation might be still be possible, an $M2$ transition is considered to be too unlikely to occur in primary gamma spectra. The choice of possible resonance spins $\mathbf{J}=\mathbf{I}+\frac{1}{2}+\mathrm{l}$ is further restricted by the s-$(\mathrm{l}=0)$ or p-wave $(\mathrm{l}=1)$ nature of the resonance. Primary transitions to different low-lying states with different spins give additional restrictions on the possible resonance spin and may lead to an unambiguous spin assignment.

However, due to Porter-Thomas fluctuations the intensities of individual primary transitions can differ greatly from the average strength of a given multipolarity. If a transition to a final state I_f is observed then J is limited to $J=I_f\pm 0,1$ but if no transition is observed, nothing can be concluded. Since these gamma rays have to be measured with high-resolution germanium detectors having a rather small detection efficiency for high-energy gamma rays, this may be problematic. For the same reason it is difficult to use the angular distribution of primary gamma radiation, although it should be mentioned that the angular distribution carries over partially to the secondary gamma radiation [30]. The uncertainty of an assignment due to a missing primary transition to a level with a given spin parity may be reduced if several primary transitions to levels with the same spin and parity are possible, e.g., to $5/2^+$ levels of ^{239}U.

III. EXPERIMENTAL SETUP

The measurements were performed at the pulsed neutron facility of the Geel Linear Electron Accelerator GELINA using the time-of-flight technique. A detailed description of the accelerator and its neutron producing target can be found elsewhere [31,32]. The Geel linac and associated compressing magnet system [33] are operated to provide electron bursts of 100 MeV average energy and 1 ns width at a maximum repetition frequency of 800 Hz and an average beam current of 60 μA. The electron beam hits a rotating uranium target, cooled by a flow of mercury. The neutrons produced via Bremsstrahlung are moderated by two slabs of 4 cm thick water canned in beryllium. After partial moderation the neutrons enter the flight paths, which are evacuated aluminum pipes of 50 cm diameter with collimators consisting of either borated wax or copper, placed at appropriate distances in order to confine the beam inside the pipe.

The neutron beam used for our gamma-ray experiments was filtered by a $^{\mathrm{nat}}B_4C$ filter of thickness 0.335 g/cm^2 to absorb the slow neutrons, as otherwise overlap with the next machine cycle will occur. In the case of the ^{238}U experiment a 1 cm thick depleted uranium disc was placed in the neutron beam. This filter served the double purpose of decreasing the intensity of the gamma flash as well as strongly reducing the count rate in the s-wave resonances and reducing the dead-time of the gamma-ray detectors. Since the peak cross sections for the ^{238}U s-wave resonances in the epithermal neutron energy region are much larger than that for the p-wave resonances, the transmission for neutrons with energies corresponding to s waves is very much reduced. In the case of the ^{113}Cd experiment, a 1 cm thick lead disc was used to decrease the gamma flash.

The samples were placed at 12.85 m from the neutron source. In the case of ^{238}U one high purity intrinsic p-type germanium detector of 70% efficiency (for the ^{60}Co lines) was used. The experiment with ^{113}Cd was done with two such detectors. The samples and the detectors were surrounded by a considerable amount of shielding, consisting of a mixture of Li_2CO_3 and wax. Directly around the sample a sleeve of ^{6}Li in an aluminum canning was used in order to moderate and absorb the neutrons scattered from the sample. The detectors were shielded against scattered neutrons by an aluminum protection cover filled with ^{6}Li and an additional 3.5 cm Li_2CO_3 on top. The whole assembly was placed inside a large shielding with walls made out of blocks of lead and a mixture of boric acid and wax, each 10 cm thick, to protect against outside radiation. The neutron flux in the center of the beam at this distance was approximately $\Phi(E)=7.0\times 10^3 E^{-0.9}$ neutrons/(cm^2 s eV). In Fig. 3 a schematic view of the setup used in the ^{238}U experiment is shown. The setup for ^{113}Cd was very similar.

The pulses of the preamplifier of the detector are used to determine the energy of the gamma ray as well as the arrival time with respect to the neutron burst, in this way giving the flight time of the neutron. For each event, the amplitude information (ADC) and the time-of-flight (TOF) information, digitized into bins with a width of 32 up to 256 ns, were accumulated by the PC-based data acquisition system and were recorded in event mode. These data were stored on an Exabyte tape unit for off-line analysis. The event-mode data are sorted in order to build gamma-ray spectra corresponding to TOF intervals of interest, i.e., the neutron resonance and background regions. A computer program, taking care of the reading and sorting of the large amount of event-mode data directly from the tape unit, has been developed [34].

The gamma-ray spectra corresponding to individual resonance capture regions were then analyzed and the positions and the areas of the gamma-ray peaks of interest were determined. The response of semiconductor detectors allows the shape of the detected gamma peaks to be adequately fitted by a Gaussian function combined with a function describing a low-energy tail. In order to obtain the pure capture yield spectrum of a given resonance, the gamma-ray spectrum of

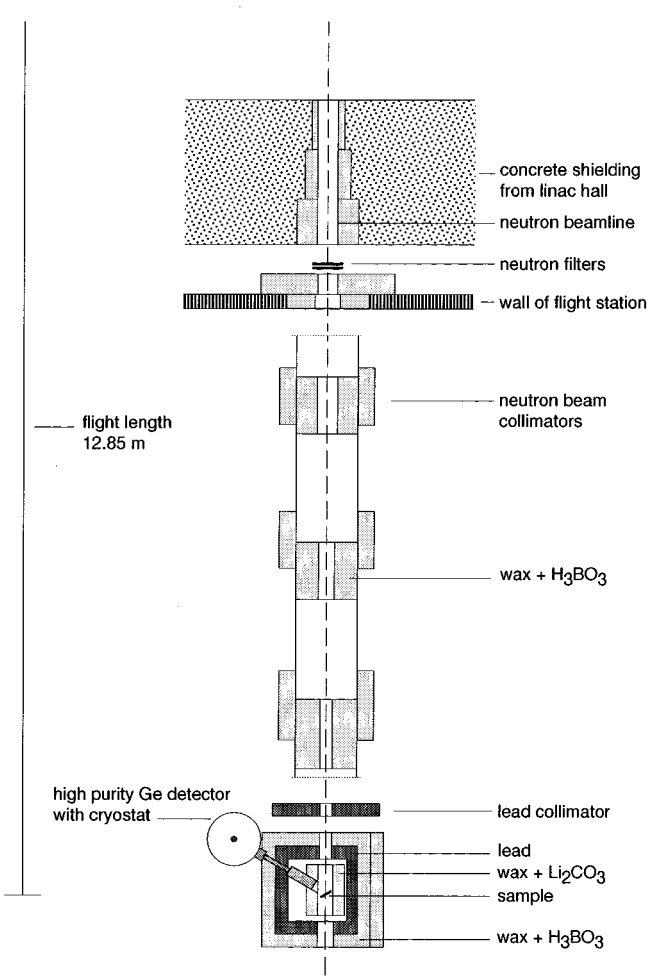

FIG. 3. Schematic view of the neutron beam line with the measurement setup.

one or more nearby background regions was subtracted from the resonance spectrum after proper data normalization.

IV. RESULTS FOR ^{238}U

A. Spin assignments

We have used a 4 mm thick very pure ^{238}U metal disc with a highly reduced ^{235}U content of 9 ppm. The sample

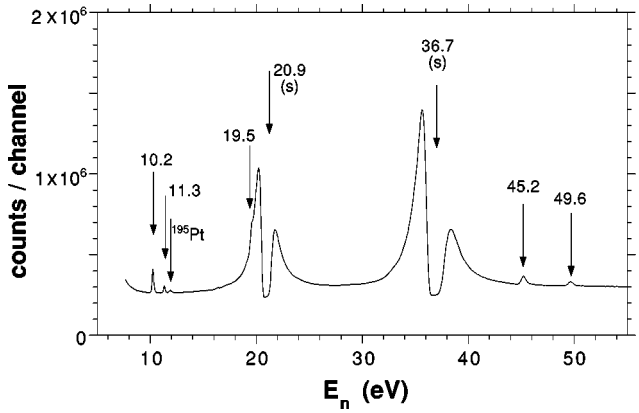

FIG. 4. Part of the time-of-flight spectrum for ^{238}U(n,γ) ^{239}U with the resonance energies indicated.

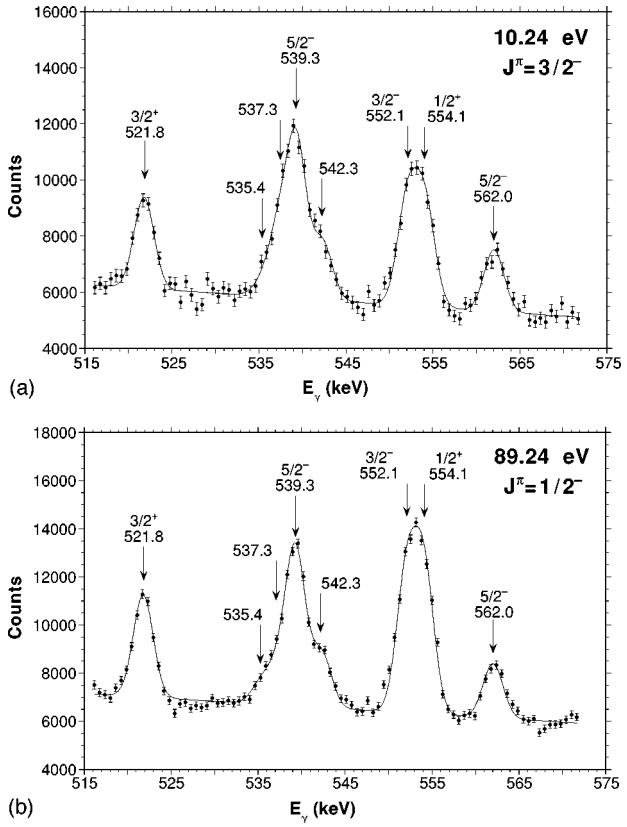

FIG. 5. Two examples of a fit of the capture gamma-ray spectrum in the 515–575 keV region for the p-wave resonances at 10.24 eV and at 89.24 eV having different spin.

having a diameter of 11.1 cm and a total weight of 694 g, was on loan from Oak Ridge National Laboratory. The thickness of the sample is accordingly 7.17 g/cm^2 or 0.0181 atoms/b. The disc has been positioned in such a way that its plane was making an angle of 60° with the neutron beam direction while the germanium detector was placed under an angle of 120°. This setup was an optimum in order to avoid self-shielding and not to reduce the time-of-flight resolution too much.

Part of the time-of-flight spectrum, corresponding to the total number of gamma-ray pulses in the energy range 0.3–5

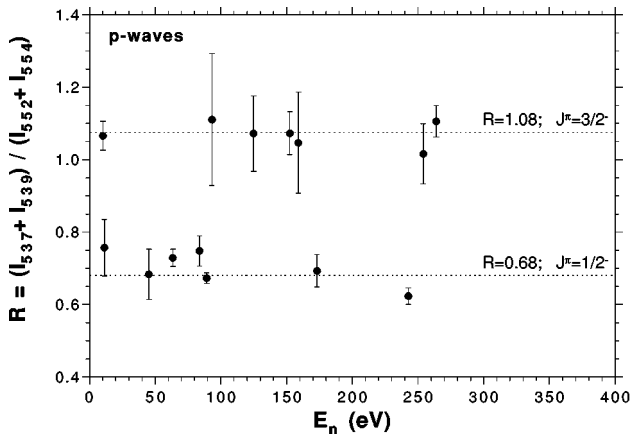

FIG. 6. The ratio $R=(I_{537}+I_{539})/(I_{552}+I_{554})$ between the sums of the intensities of the indicated gamma rays plotted against energy for 14 p-wave resonances of ^{238}U(n,γ).

TABLE I. Experimental intensities, in photons per 100 neutrons captured, of primary gamma-ray transitions leading to $J^\pi = 5/2^+$ states in ^{239}U.

E_γ					E_n (eV)				
(keV)	10.24	19.53	93.14	98.20	253.9	263.9	282.5	351.9	439.7
4806.4	0.41±	>0.45			1.63±	1.34±	1.81±	5.44±	>0.89
$\rightarrow 5/2^+$	0.08				0.33	0.25	0.33	0.93	
4612.5				2.19±	3.60±	0.81±	1.68±	2.65±	>0.71
$\rightarrow 5/2^+$				0.45	0.65	0.18	0.33	0.59	
4049.7		>0.70	0.61±						
$\rightarrow 5/2^+$			0.15						
3744.0	0.19±								
$\rightarrow 5/2^+$	0.04								

MeV, is plotted against the neutron energy in Fig. 4. The ''self-indication'' technique of the uranium filter in the neutron beam results in a dip in the observed peak of strong resonances in the capture spectrum. One should note the absence of any isotopic structure other than due to ^{238}U(n,γ) thanks to the extremely low contents of ^{235}U and to the efficient absorption of scattered neutrons. A very small structure at 11.9 eV shows up in the time-of-flight spectrum. We have identified it as a resonance of ^{195}Pt(n,γ) by means of its characteristic gamma rays. This is presumably related to platinum introduced as an impurity during the production of the sample. No other peaks due to impurities were observed.

A resonance at 57.9 eV was observed in a preliminary measurement with a sample containing 2000 ppm ^{235}U but was not observed using a sample with only 9 ppm ^{235}U. We conclude that there is no resonance at this energy in ^{238}U but that the observed structure, previously attributed to ^{238}U, is due to a neighboring well-known resonance in ^{235}U.

TABLE II. The spin assignments for 19 p-wave resonances in ^{238}U(n,γ).

E_0(eV)	Low-level population	Primary transitions	Adopted
10.24	3/2	3/2	3/2
11.31	1/2		1/2
19.53		3/2	3/2
45.17	1/2		1/2
63.52	1/2		1/2
83.68	1/2		1/2
89.24	1/2		1/2
93.14	3/2	3/2	3/2
98.20		3/2	3/2
124.97	3/2		3/2
152.42	3/2		3/2
158.98	3/2		3/2
173.18	1/2		1/2
242.73	1/2		1/2
253.90	3/2	3/2	3/2
263.94	3/2	3/2	3/2
282.46		3/2	3/2
351.86		3/2	3/2
439.75		3/2	3/2

We collected in total 18 Gbyte of event-mode data during 1200 h of effective beam time. From these data 79 gamma-ray spectra of 8192 channels corresponding to as many time-of-flight intervals were sorted out, each being associated with an s-wave, a p-wave resonance, or a ''background'' region in between resonances. For the gamma-ray spectra an accurate energy calibration as well as a determination of the full width at half maximum (FWHM) of the peaks was obtained from nearby resolved peaks belonging to spectra with high counting statistics, typically s-wave resonances. Then both peak positions as well as their widths were kept fixed in the fitting of the gamma-ray spectra of the p-wave resonances. For some p-wave resonances which are located on the shoulder of a nearby s-wave resonance, the yield was fitted with the program REFIT [35] in order to determine and correct for the fraction of s-wave capture in the given TOF interval. This was the case for the p-wave resonances at 63.52, 83.68, 98.20, 124.97, 242.73, and 351.86 eV.

Sections of the gamma-ray spectra of the two most intense p-wave resonances at 10.24 and 89.24 eV are shown in Fig. 5. The data in the 515–575 keV region are fitted with eight known transitions. At the top of each peak the energy and the spin and parity of the deexcited state, taken from the literature [36,37], are shown. Since the effective resolution of our germanium detector at these lines was about 2.7 keV FWHM, it is not possible to resolve all transitions. One may notice that in the upper part of Fig. 5 the doublet dominated by the 539 keV line, from a $J^\pi = 5/2^-$ state, is higher than

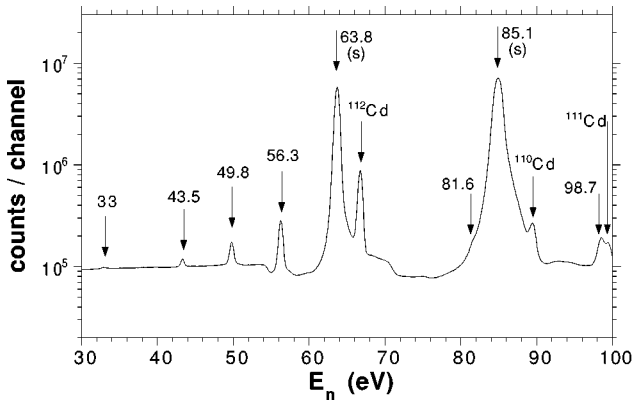

FIG. 7. Part of the time-of-flight spectrum for ^{113}Cd(n,γ) ^{114}Cd on a logarithmic scale with the resonance energies indicated.

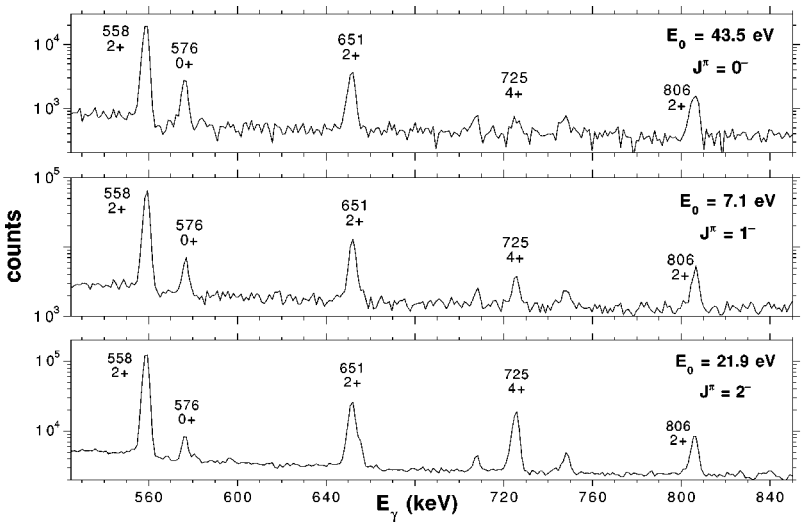

FIG. 8. Three examples of capture gamma-ray spectra in the 525–850 keV energy region for the first tree p-wave resonances of ^{113}Cd(n,γ) having different spins.

the multiplet at 552–554 keV, deexciting states with $J^\pi = 1/2^+, 3/2^-$. In the lower part it is the opposite. Because it should be clear from what has been discussed in the second section that a 5/2 state is populated more by a 3/2 capture state than by a 1/2 state, we assigned $J^\pi = 3/2^-$ to the 10.24 eV resonance and $J^\pi = 1/2^-$ to the 89.24 eV resonance. These assignments were confirmed by the information of the primary gamma rays. A strong 4806 keV transition to the $5/2^+$ ground state is present in the case of the 10.24 eV resonance. This gamma ray has also been observed by Wasson *et al.* [38] who assigned $J^\pi = 3/2^-$ for this resonance. This transition is not visible in the 89.24 eV resonance.

In order to divide the resonances into two spin groups, we calculated the ratio R of the intensities of the two doublets $R = (I_{537} + I_{539})/(I_{552} + I_{554})$ for those resonances having sufficient statistics. In fact, the gamma ray at 554 keV is also a very close doublet, consisting for 80% of the decay of the $J^\pi = 1/2^+$ level at 687.88 keV while the remaining fraction is the decay of the $J^\pi = 1/2^-$ or $3/2^-$ level at 1242 keV. In Fig. 6 this ratio R is plotted for the different p-wave resonances. This figure shows a splitting of the ratios into two groups for the p-wave resonances. The weighted averages of the ratios for each group are shown by the two horizontal lines which can be associated to the $J = 1/2$ and the $J = 3/2$ resonances.

In the high-energy gamma-ray spectra which were also investigated in p-wave resonances of ^{238}U, four primary transitions at 4806.4, 4612.5, 4049.7, and 3744.0 keV, leading to $J^\pi = 5/2^+$ states, were observed in some of them.

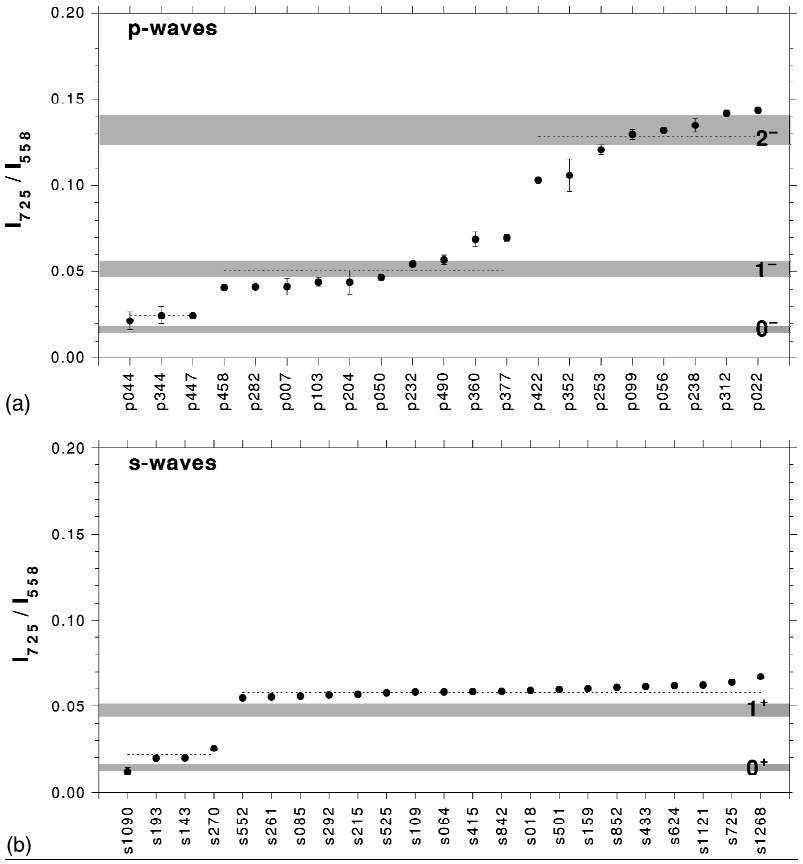

FIG. 9. The ratio of the intensities of the 725 and the 558 keV gamma rays, for both the s-wave and p-wave resonances, in increasing order. The dotted lines indicate the weighted mean of each spin group. The gray bands are the results of simulations [22].

These transitions have $E1$ multipolarity for initial states with $J^\pi = 3/2^-$ and $M2$ multipolarity for a $J^\pi = 1/2^-$ resonance. In the second case the transitions are expected to be several orders of magnitude weaker and therefore not observable. In this way we can identify only $3/2^-$ states; the absence of such transitions is not a complete guarantee for a $1/2^-$ state, due to the Porter-Thomas fluctuations of the gamma transitions.

We derived the approximate relative intensities of the primary gamma rays by assuming that the experimentally measured resonance capture area is proportional to the capture cross section. This assumption is justified because the gamma-energy range covers the whole spectrum except for the first 300 keV and also because the sample is thin. Thus the area of a primary gamma ray divided by the total number of counts in the resonance is in good approximation proportional to the intensity of the gamma ray. To obtain the absolute intensities one can find the normalization constant using well-known intensities from the literature. The areas of the mentioned peaks were fitted and the corresponding intensities normalized to those given in [38] for the 20.87 eV s-wave resonance. A list of the normalized intensities, expressed in photons per 100 neutrons captured, is given in Table I for nine p-wave resonances which were, on this basis, assigned as $J=3/2$ p-wave resonances. For two resonances which could not be corrected satisfactorily for the strong contamination of s-wave capture, we give only a lower limit of the intensities. The resulting spin assignments are summarized in Table II, showing the assignments based on the low-level population method and on information from primary transitions, both in complete agreement with each other.

B. Estimation of M

Spin assignments can be used to refine the estimate of the root mean square parity nonconserving matrix element M using the experimental PNC effects. The importance of knowing the spins in such an estimation procedure has been recently demonstrated [39,40].

It is supposed that in the approach of the statistical model the PNC matrix elements form a random variable with a Gaussian distribution within the ensemble of p-wave resonances that can show PNC. To extract the width of this distribution from the measured PNC asymmetries, i.e., the root mean square parity nonconserving matrix element M, it is important to know which of the p-wave resonances can be admixed by which s-wave resonances. In a spin-zero target nucleus like ^{238}U, only the $J=1/2$ p-wave resonances can be admixed by the $J=1/2$ s waves while the $J=3/2$ p waves cannot. The measured asymmetries of the $J=3/2$ should therefore be consistent with zero. For large asymmetries it is obvious that the p-wave resonance should have $J=1/2$. For smaller asymmetries, it is not clear if it is a real asymmetry or if it is zero within the error. Therefore, for a proper estimation of M it is necessary to include the spin information in order to reduce the uncertainty of the estimate and to reduce the bias of the estimate. For a target nucleus with a spin unequal to zero, there are more possible values of the spin for both s-wave and p-wave resonances and the parity nonconserving mixing is more involved [40,41].

We will not elaborate on the estimation of the root mean square parity nonconserving matrix element M for ^{238}U here, as the latest published data for the measured asymmetries are likely to be updated in the near future [5]. We only like to mention that the maximum likelihood procedure with the inclusion of known spins shows a substantial decrease in the uncertainty of the estimate [39].

V. RESULTS FOR ^{113}Cd

In this experiment we used a highly enriched ^{113}Cd metal disc (93.35%) of 90 mm diameter, 1.65 mm thick, and with a total weight of 91.2 g. The sample was obtained from the Russian State Pool of Isotopes. The thickness of the sample was 1.434 g/cm^2 or 0.00764 atoms/b. Also this sample was placed at the 12.85 m flight distance, but now perpendicular to the neutron beam and viewed by two coaxial intrinsic germanium detectors of 70% efficiency, both placed at opposite sides of the sample. The time and amplitude information from the detectors was processed in the same way as in the case of ^{238}U. We collected an amount of 20 Gbyte of raw data during 700 h of effective beam time. The data were sorted into 150 gamma-ray spectra corresponding to TOF intervals associated with resonance and background regions for both detectors. In Fig. 7 part of the time-of-flight spectrum, i.e., the total number of gamma-ray pulses corresponding to $0.3<E_\gamma<9.0$ MeV collected into 32–256 ns wide time bins, is plotted as a function of the neutron energy on a logarithmic scale to make appear the small p-wave resonances. Characteristic gamma rays made clear that several weak resonances belonged to other Cd isotopes. Resonances of the even-odd nucleus ^{111}Cd could be distinguished by their 617 keV gamma ray, while resonances from the even-even isotopes ^{110}Cd, ^{112}Cd, and ^{114}Cd were identified by means of characteristic gamma rays in the 300–500 keV energy range. Recently, Frankle *et al.* identified 23 p-wave resonances in ^{113}Cd in the neutron energy range up to 500 eV [42].

The gamma-ray spectra corresponding to the resonance regions have been corrected for the background. The areas of several peaks of interest have been fitted with both a symmetric Gaussian peak shape and with an asymmetric peak shape for the two detectors. Low-energy capture gamma-ray spectra in the 525–850 keV region are plotted on a logarithmic scale in Fig. 8 for the three p-wave resonances at 7.1, 21.9, and 43.5 eV and with apparently different spins. The energies of five transitions and the J^π values of the corresponding initial states are given above each peak. The intensity of the strong 558 keV transition, presumably little affected by the initial spin value, can be considered in the first approximation as a measure of the number of neutrons captured in a given resonance. About 70% of all decays pass through this first excited (2^+) state. Compared to that, the intensity of the 725 keV transition, from a 4^+ level, increases with increasing value of the resonance spin. On the contrary, the 576 keV line, from a 0^+ level, decreases with increasing value of the spin of the resonance state. This behavior is in agreement with the basic assumption of the present spin assignment method, namely that the population of a given low-lying state increases when the difference between its spin and that of the resonance decreases. The cor-

TABLE III. Experimental intensities, in photons per 10 000 neutrons captured, of primary gamma-ray transitions leading to $J^{\pi}=0^{+}$ and 3^{+} states in ^{114}Cd.

E_{γ}	E_n (eV)										
(keV)	7.1	21.9	49.8	56.3	102.5	232.4	282.0	312.4	359.5	377.0	457.9
9043	42.2±		96.1±						36.6±		94.3±
$\rightarrow 0^{+}$	8.7		5.9						28.3		8.1
7908	29.5±		48.6±		18.0±	6.8±				42.8±	94.4±
$\rightarrow 0^{+}$	10.4		5.4		6.0	1.8				18.4	7.8
7737	24.5±				32.7±		104.8±				148.5±
$\rightarrow 0^{+}$	9.7				12.7		9.4				10.2
7183											75.9±
$\rightarrow 0^{+}$											15.2
7179		43.8±									
$\rightarrow 3^{+}$		5.0									
6838				32.3±				39.4±			
$\rightarrow 3^{+}$				3.2				13.0			

responding spectra for the 0^{+} and the 1^{+} s-wave resonances are very similar to those of the 0^{-} and the 1^{-} p waves.

Several ratios of the intensities of gamma rays have been calculated for each group of resonances. We have studied the ratios of gamma rays depopulating states with different spin, notably those of 576, 651, 725, 806, and 1400 keV. In the case of s-wave resonances, due to the good statistics, the values of each ratio split up clearly into two groups and the results of the spin assignments obtained by the various ratios are entirely consistent with each other. In the case of p-wave resonances, where, due to counting statistics, background and contamination from nearby resonances are more important, not all studied gamma intensity ratios gave a clear splitting into three groups. We found that the ratio

TABLE IV. The spin assignments for 23 s-wave and 21 p-wave resonances in ^{113}Cd(n,γ). The asterisk refers to [11].

s-wave resonances		p-wave resonances			
E_0(eV)	Low-level population	E_0(eV)	Low-level population	Primary transitions	Adopted
*18.41	1	7.08	1	1	1
*63.82	1	21.91	2	2	2
*85.13	1	43.50	0		0
*108.5	1	49.81	1	1	1
143.2	0	56.32	2	2	2
158.8	1	98.7	2		2
*192.9	0	102.5	1	1	1
*215.4	1	203.6	1		1
*261.2	1	232.4	1	1	1
*269.6	0	237.9	2		2
291.8	1	252.7	2		2
*414.5	1	282.0	1	1	1
*432.5	1	312.4	2	2	2
501.3	1	343.9	0		0
*525.3	1	351.7	2		2
*552.2	1	359.5	1	1	1
624.3	1	377.0	1	1	1
724.8	1	422.3	2		2
842.4	1	447.3	0		0
*851.9	1	457.9	1	1	1
1089.9	0	490.1	1		1
1120.9	1				
*1268.4	1				

$R=I_{725}/I_{558}$ was the most useful. To distinguish the different groups clearly, we have plotted the ratios R in Fig. 9 in increasing order so that a gap on the y ordinate indicates a change of spin group. As the number of groups into which the data will split is known *a priori*, two groups for the s waves and three groups for the p-wave resonances, this treatment is justified. There is still a spread in each spin group due to a complex variety of influences from contributions of background and other resonances and due to the fact that the gamma decay is not an entirely statistical process but that still some structure effects may favor specific gamma cascades.

We have used the computer code DICEBOX [21] to simulate the process of statistical gamma cascade deexcitation of ^{113}Cd [22]. The program generates sets of levels in the quasicontinuum region of the excitation spectrum according to a given level density formula and generates also a corresponding full set of partial radiative widths. An event consists of the gamma decay of the highly excited resonance state through intermediate levels to a level in the discrete level region. In this way, the population of the levels in the discrete level region is simulated. The known branching ratios in this region allow one to calculate a gamma-ray spectrum that can be compared with the experimental spectra. The event-by-event basis of the program allows a rigorous inclusion of the Porter-Thomas fluctuations of the individual gamma-ray intensities. The gray bands that are also shown in Fig. 9 correspond to the one sigma intervals of the ratio $R=I_{725}/I_{558}$ obtained by simulations.

Strong primary gamma transitions to 0^+ and 3^+ states have been observed in several p-wave resonances, indicating $E1$ transitions from 1^- and 2^- resonances respectively. Because the low-lying states in ^{114}Cd are well separated, also the primary transitions populating them are distinctly spaced and therefore adequately identifiable. Indications for 2^- resonances were obtained from the gamma rays of 7179 and 6838 keV, leading to 3^+ states. Gamma rays of 9043, 7908, 7737, and 7183 keV, transitions to 0^+ states, indicate 1^- p-wave resonances.

We derived the absolute intensities by normalizing to the total capture rate. We used a method, described by Coceva [43], that consists of determining the relative intensities A_{j0} of all gamma rays that populate the ground state and measuring the relative efficiency $\epsilon(E_{\gamma j0})$. Then, the absolute intensity $I_{\gamma if}$ of a primary transition $i\rightarrow f$ is expressed as

$$I_{\gamma if}=\frac{\Gamma_{\gamma if}}{\Gamma_{\gamma i}}=\frac{A_{if}/\epsilon(E_{\gamma i0})}{\Sigma_j A_{j0}/\epsilon(E_{\gamma j0})}. \quad (2)$$

In Table III the absolute intensities of primary gamma rays, expressed in photons per 10^4 neutrons captured, are given together with the estimated uncertainties. The assigned spins are summarized in Table IV for 23 s-wave resonances and 21 p-wave resonances. The spins of s-wave resonances indicated with an asterisk were already known from [11]. The agreement is perfect. The spins for the p-wave resonances obtained with the low-level population method and with the use of primary gamma rays are completely consistent with each other.

VI. CONCLUSION

The spin assignment method applied in the experiments described here, the low-level population method, is well suitable to assign neutron resonance spins for medium and heavy mass nuclei. The method was already known for its use in the case of s-wave resonances and has now thoroughly been established as a powerful method for spin assignments of p-wave resonances which are on the average a factor 1000 weaker than s-wave resonances in the epithermal neutron energy range. In addition, the observation of primary gamma transitions to levels with known spins has given additional information about resonance spins.

Spins have been successfully assigned to 19 neutron p-wave resonances of ^{238}U, of which seven were found to be $J=1/2$. In the case of ^{113}Cd, spins of 23 neutron s-wave resonances as well as 21 p-wave resonances have been determined. The knowledge of the spins of neutron resonances is important for the analysis of PNC measurements.

ACKNOWLEDGMENTS

The authors want to thank H. Weigmann for valuable discussions, M. C. Moxon for his help with REFIT, F. Bečvář and P. Cejnar for their help and cooperation with DICEBOX, and P. ter Meer for his assistance in informatics. We also thank Oak Ridge National Laboratory for the loan of the high purity ^{238}U sample.

[1] V. P. Alfimenkov, S. B. Borzakov, V. V. Thuan, Y. D. Mareev, L. B. Pikelner, A. S. Khrykin, and E. I. Sharapov, Nucl. Phys. **A398**, 93 (1983).

[2] X. Zhu, J. D. Bowman, C. D. Bowman, J. E. Bush, P. P. J. Delheij, C. M. Frankle, C. R. Gould, D. G. Haase, J. N. Knudson, G. E. Mitchell, S. Penttil, H. Postma, N. R. Roberson, S. J. Seestrom, J. J. Szymanski, and V. W. Yuan, Phys. Rev. C **46**, 768 (1992).

[3] C. M. Frankle, J. D. Bowman, J. E. Bush, P. P. J. Delheij, C. R. Gould, D. G. Haase, J. N. Knudson, G. E. Mitchell, S. Penttil, H. Postma, N. R. Roberson, S. J. Seestrom, J. J. Szymanski, S. H. Yoo, V. W. Yuan, and X. Zhu, Phys. Rev. C **46**, 778 (1992).

[4] S. J. Seestrom, D. Alde, J. D. Bowman, B. E. Crawford, P. P. J. Delheij, C. M. Frankle, K. Fukuda, C. R. Gould, A. A. Green, D. G. Haase, M. Iinuma, J. N. Knudson, L. Y. Lowie, A. Masaike, Y. Masuda, Y. Matsuda, G. E. Mitchell, S. Penttild, S. Stephenson, Yu. P. Popov, H. Postma, N. R. Roberson, E. I. Sharapov, H. Shimizu, Y. F. Yen, and V. W. Yuan, *Proceedings of the 2nd International Seminar on Interaction of Neutrons with Nuclei* (Joint Institute for Nuclear Research, Dubna, 1994), p. 50.

[5] G. E. Mitchell, in *Capture Gamma-Ray Spectroscopy and Related Topics 1996*, edited by G. L. Molnar, T. Belgya, and Zs. Revay (Springer, Budapest, 1997).

[6] F. Corvi, F. Gunsing, K. Athanassopulos, H. Postma, and A.

Mauri, in *Time Reversal Invariance and Parity Violation in Neutron Reactions*, edited by C. R. Gould, J. D. Bowman, and Yu. P. Popov (World Scientific, Singapore, 1994), p. 79.

[7] F. Gunsing, F. Corvi, K. Athanassopulos, H. Postma, and A. Mauri, in *Capture Gamma-Ray Spectroscopy and Related Topics*, edited by J. Kern (World Scientific, Singapore, 1994), p. 797.

[8] F. Gunsing, F. Corvi, K. Athanassopulos, H. Postma, Yu. P. Popov, and E. I. Sharapov, *Neutron Spectroscopy, Nuclear Structure, Related Topics* (Joint Institute for Nuclear Research, Dubna, 1994), p. 162.

[9] F. Gunsing, Ph.D. thesis, Delft University, 1995.

[10] L. Zanini, F. Corvi, K. Athanassopulos, H. Postma, and F. Gunsing, in *Capture Gamma-Ray Spectroscopy and Related Topics 1996* [5].

[11] S. F. Mughabghab, M. Divadeenam, and N. E. Holden, *Neutron Cross Sections: Neutron Resonance Parameters and Thermal Cross Sections* (Academic Press, New York, 1981).

[12] G. A. Keyworth, C. E. Olsen, F. T. Seibel, J. W. T. Dabbs, and N. W. Hill, Phys. Rev. Lett. **31**, 1077 (1973).

[13] E. R. Reddingius, H. Postma, C. E. Olsen, D. C. Rorer, and V. L. Sailor, Nucl. Phys. **A218**, 84 (1974).

[14] M. S. Moore, J. D. Moses, G. A. Keyworth, J. W. T. Dabbs, and N. W. Hill, Phys. Rev. C **18**, 1328 (1978).

[15] H. Postma, *Proceedings of the 2nd International Seminar on Interaction of Neutrons with Nuclei* [4], p. 170.

[16] C. Coceva, F. Corvi, and P. Giacobbe, Nucl. Phys. **A117**, 586 (1968).

[17] G. P. Georgiev, Y. V. Grigoriev, G. V. Muradyan, and N. B. Yaneva, *Capture Gamma-Ray Spectroscopy and Related Topics* (World Scientific, Fribourg, 1993), p. 581.

[18] H. Postma, Phys. Rev. C **24**, 2322 (1981).

[19] A. Gilbert and A. G. W. Cameron, Can. J. Phys. **43**, 1446 (1965).

[20] T. v. Egidy, H. H. Schmidt, and A. N. Behkami, Nucl. Phys. **A481**, 189 (1988).

[21] F. Bečvář and S. Ulbig, DICEBOX, computer code, Charles University, Prague, 1991.

[22] F. Gunsing, F. Corvi, H. Postma, and Bečvár, Nucl. Instrum. Methods Phys. Res. A **365**, 410 (1995).

[23] L. Zanini, Ph.D. thesis, Delft University, in preparation.

[24] F. Corvi, L. Zanini, H. Postma, and F. Gunsing, unpublished.

[25] K. J. Wetzel and G. E. Thomas, Phys. Rev. C **1**, 1501 (1970).

[26] W. P. Poenitz and J. R. Tatarczuk, Nucl. Phys. **A151**, 569 (1970).

[27] M. R. Bhat, R. E. Chrien, D. I. Garber, and O. A. Wasson, Phys. Rev. C **2**, 1115 (1970).

[28] F. Corvi, M. Stefanon, C. Coceva, and P. Giacobbe, Nucl. Phys. **A203**, 145 (1973).

[29] L. Aldea, F. Bečvář, H. T. Hiep, S. Pospisil, and S. A. Telezhnikov, Czech. J. Phys. B **28**, 17 (1978).

[30] H. Postma and J. F. M. Potters, Physica (Amsterdam) **45**, 559 (1970).

[31] J. M. Salomé and R. Cools, Nucl. Instrum. Methods **179**, 13 (1981).

[32] J. M. Salomé, Physicalia **8**, 261 (1986).

[33] D. Tronc, J. M. Salomé, and K. H. Böckhoff, Nucl. Instrum. Methods Phys. Res. A **228**, 217 (1985).

[34] F. Gunsing, P. ter Meer and C. Cervini, DATASORT, computer code, Macintosh Scientific and Technical Users Association, Inc., CD-ROM, 1993.

[35] M.C. Moxon and J.B. Brisland, REFIT, *A least squares fitting program for resonance analysis of neutron transmission and capture data computer code* (United Kingdom Atomic Energy Authority, Harwell, 1991).

[36] A. Mheemeed, K. Schreckenbach, G. Barreau, H. R. Faust, H. G. Brner, R. Brissot, P. Hungerford, H. H. Schmidt, H. J. Scheerer, T. v. Egidy, K. Heyde, J. L. Wood, P. v. Isacker, M. Waroquier, and G. Wenes, Nucl. Phys. **A412**, 113 (1984).

[37] J. Blachot and G. Marguier, Nucl. Data Sheets **60**, 139 (1990).

[38] O. A. Wasson, R. E. Chrien, G. G. Slaughter, and J. A. Harvey, Phys. Rev. C **4**, 900 (1971).

[39] H. Postma, F. Gunsing, and F. Corvi, Phys. Rev. C **53**, 558 (1996).

[40] J. D. Bowman, L. Y. Lowie, G. E. Mitchell, E. I. Sharapov, and Yi-Fen Yen, Phys. Rev. C **53**, 285 (1996).

[41] H. Postma, J. D. Bowman, B. E. Crawford, F. Corvi, P. P. J. Delhey, F. Gunsing, T. Haseyama, J. N. Knudson, L. Y. Lowie, A. Masaike, Y. Masuda, Y. Matsuda, G. E. Mitchell, S. Penttila, N. R. Roberson, S. J. Seestrom, E. I. Sharapov, H. M. Shimizu, S. L. Stephenson, Y. F. Yen, V. W. Yuan, and L. Zanini, *Proceedings 4th International Seminar on Interaction of Neutrons with Nuclei* (Joint Institute for Nuclear Research, Dubna, 1996), p. 101.

[42] C. M. Frankle, C. D. Bowman, J. D. Bowman, S. J. Seestrom, E. I. Sharapov, Y. P. Popov, and N. R. Roberson, Phys. Rev. C **45**, 2143 (1992).

[43] C. Coceva, Nuovo Cimento A **107**, 85 (1994).